Original Research *Highlight article*

Comprehensive analysis of INHBA: A biomarker for anti-TGFβ treatment in head and neck cancer

Shunhao Zhang[1], Keyu Jin[1], Tianle Li[1], Maolin Zhou[1] and Wenbin Yang[2]

[1]State Key Laboratory of Oral Diseases, National Clinical Research Center for Oral Diseases, West China Hospital of Stomatology, Sichuan University, Chengdu 610041, China; [2]State Key Laboratory of Oral Diseases, National Clinical Research Center for Oral Diseases, Department of Oral and Maxillofacial Surgery, Department of Medical Affairs, West China Hospital of Stomatology, Sichuan University, Chengdu 610041, China
Corresponding author: Wenbin Yang. Email: yangwenbinkq@163.com

Impact Statement

Head and neck squamous cell carcinoma (HNSC) is one of the most common causes of cancer-related deaths worldwide. *INHBA* is a protein-coding gene belonging to the transforming growth factor β (TGFβ) superfamily, and many studies have shown that *INHBA* dysregulation is associated with the progression of various cancers. However, the role of *INHBA* in HNSC remains unclear. Exploring the expression profile of *INHBA* and its prognostic implications in HNSC are critical. Here, we reveal that *INHBA* upregulation is significantly associated with poor overall survival (OS) and disease-free survival (DFS) in HNSC. Multivariate Cox regression revealed that *INHBA* overexpression is an independent poor prognostic factor in HNSC, and the *INHBA*-based prognostic model has a more powerful predictive ability than tumor–node–metastasis (TNM) staging system alone. In addition, copy number alterations and miR-217-5p downregulation are potential mechanisms for elevated *INHBA* expression in HNSC. In summary, *INHBA* may represent a promising predictive biomarker and candidate target for anti-TGFβ therapy in HNSC.

Abstract

Inhibin subunit βA (*INHBA*) is a protein-coding gene belonging to the transforming growth factor β (TGFβ) superfamily, which is associated with the development of a variety of cancers. However, the role of *INHBA* in head and neck squamous cell carcinoma (HNSC) remains unclear. The expression profile and prognostic significance of *INHBA* in HNSC were assessed using a variety of informatics methods. The level of *INHBA* expression was significantly higher in patients with HNSC, and it was correlated with sex, tumor–node–metastasis (TNM) stage, histological grade, and human papillomavirus (HPV) status. Kaplan–Meier (K–M) analysis indicated that poor overall survival (OS) and disease-free survival (DFS) were significantly associated with *INHBA* upregulation in HNSC. *INHBA* overexpression was validated as an independent poor prognostic factor by multivariate Cox regression, and including *INHBA* expression level in the prognostic model could increase prediction accuracy. In addition, copy number alterations (CNAs) of *INHBA* and miR-217-5p downregulation are potential mechanisms for elevated *INHBA* expression in HNSC. In conclusion, *INHBA* may represent a promising predictive biomarker and candidate target for anti-TGFβ therapy in HNSC.

Keywords: INHBA, head and neck squamous cell carcinoma, copy number alterations, miR-217-5p, prognostic model, TGFβ

Experimental Biology and Medicine **2022; 247: 1317–1329. DOI: 10.1177/15353702221085203**

Introduction

Head and neck squamous cell carcinoma (HNSC), comprising the majority of primary head and neck cancers, is the third most common malignancy and the seventh leading cause of cancer-related deaths worldwide, with a global occurrence of 750,000 cases annually.[1,2] Despite significant advances in the diagnosis and treatment of HNSC, the high rate of metastasis (approximately 65% of patients) and unfavorable prognosis (5-year survival rate of <50%) highlight the importance of further research into the molecular biology and pathogenesis mechanisms of HNSC.[3,4] Furthermore, because aberrant gene expression profiles that characterize tumor biological activities are well recognized as activators of cancer formation and progression, discovering new therapeutic targets to improve early diagnosis and comprehensive therapy of HNSC is of significant interest.

The transforming growth factor β (TGFβ) pathway is a pleiotropic signaling cascade mediating various molecular and cellular processes, whose dysregulation is responsible

for carcinogenesis and cancer progression in different tissue types due to increased genomic instability.[5] Canonical TGFβ signaling begins with TGF-β receptor II (TGFβRII)-mediated ligand binding, which subsequently phosphorylates TGFβ receptor I (TGFβRI) and results in the phosphorylation of receptor-activated Smads (R-Smads). Phosphorylated R-Smads then translocate to the nucleus to either directly bind Smad binding elements to regulate gene expression or form complexes with common Smad (Co-Smad). The TGFβ pathway can be attenuated by inhibitory Smads by recruiting ubiquitin ligases to degrade R-Smads and TGFβRI or by competing with R-Smads to bind TGFβRI.[6] Non-canonical signaling pathways, such as phosphatidylinositol 3-kinase (PI3K)-protein kinase B (AKT), p38 mitogen-activated protein kinase (MAPK), c-Jun N-terminal kinase (JNK), and nuclear factor-kappa B (NF-κB) activated by TGFβ, are correlated with tumor progression.[7] Activin A, a TGFβ superfamily ligand encoded by the inhibin subunit βA (*INHBA*) gene, is best characterized for its critical role in the hypothalamus–pituitary gland–gonad axis and regulating the development of testes, teeth, and eyes under normal physiological circumstances.[8,9] In the case of activin A, the signaling pathway is triggered by active activin A binding to activin receptor types II and IIB (ActRII/IIB), which recruits ALK4 and activates the Smad-dependent signaling cascade similar to the TGFβ pathway.[10] In addition to its physiological functions, many studies have found multiple roles of *INHBA* in various cancers, including HNSC. Indeed, Chang *et al.* reported that downregulation of miR-376c and subsequent dysregulation of the *RUNX2*/*INHBA* axis promotes lymph node metastasis in HNSC.[11] Tsai *et al.* indicated that activation of the epidermal growth factor receptor (EGFR) promoter by activin A is essential for the carcinogenesis of oral cavity squamous cell carcinoma (OSCC).[12] Data mining has also revealed the potential role of *INHBA* as a novel biomarker for HNSC.[13] Although these findings strongly support the pivotal role of *INHBA* in HNSC, the current knowledge about the mechanism of *INHBA* regulation and its prognostic significance compared to markers used in standard settings remains limited.

Therefore, we used integrated bioinformatics analysis and *in vitro* validation to determine the expression pattern of *INHBA* and its therapeutic potential in HNSC. We also sought to explore the biological functions of *INHBA* and the potential mechanisms of *INHBA* dysregulation in HNSC. Accumulating evidence suggests that miR-217-5p acts as a tumor regulator, inhibits cancer proliferation and metastasis, and promotes apoptosis by binding to target genes.[14] Therefore, we investigated the interaction between *INHBA* and miR-217-5p and discovered a significantly correlated expression pattern with a putative binding site.

Materials and methods

Data acquisition

Clinical data, messenger RNA (mRNA) sequencing data, and micro RNA (miRNA) sequencing data of patients with HNSC and normal controls were retrieved from The Cancer Genome Atlas (TCGA)-HNSC data set. The primary sites of HNSC were as follows: (1) base of tongue; (2) bones, joints, and articular cartilage of other and unspecified sites; (3) floor of mouth; (4) gum; (5) hypopharynx; (6) larynx; (7) lip; (8) oropharynx; (9) other and ill-defined sites in the lip, oral cavity, and pharynx; (10) other and unspecified parts of the mouth; (11) other and unspecified parts of the tongue; (12) palate; and (13) tonsil. The *R* package edgeR was used to normalize the raw count data and identify differentially expressed genes between HNSC tissues and normal controls. The statistical significance level was set at 0.05, with $|\log_2 FC| > 1$. In addition, *INHBA* expression profiles in several tumor tissues and paired normal tissues were explored using gene expression profiling interactive analysis (GEPIA),[15] and the tumor types were as follows: adrenocortical carcinoma (ACC), bladder urothelial carcinoma (BLCA), breast invasive carcinoma (BRCA), cervical squamous cell carcinoma and endocervical adenocarcinoma (CESC), cholangio carcinoma (CHOL), colon adenocarcinoma (COAD), lymphoid neoplasm diffuse large B-cell lymphoma (DLBC), esophageal carcinoma (ESCA), glioblastoma multiforme (GBM), HNSC, kidney chromophobe (KICH), kidney renal clear cell carcinoma (KIRC), kidney renal papillary cell carcinoma (KIRP), acute myeloid leukemia (LAML), brain lower grade glioma (LGG), liver hepatocellular carcinoma (LIHC), lung adenocarcinoma (LUAD), lung squamous cell carcinoma (LUSC), mesothelioma (MESO), ovarian serous cystadenocarcinoma (OV), pancreatic adenocarcinoma (PAAD), pheochromocytoma and paraganglioma (PCPG), prostate adenocarcinoma (PRAD), rectum adenocarcinoma (READ), sarcoma (SARC), skin cutaneous melanoma (SKCM), stomach adenocarcinoma (STAD), testicular germ cell tumors (TGCT), thyroid carcinoma (THCA), thymoma (THYM), Uterine corpus endometrial carcinoma (UCEC), uterine carcinosarcoma (UCS), and uveal melanoma (UVM). While *INHBA* copy number alterations (CNAs), DNA methylation, and the relationship between *TP53* mutations and *INHBA* expression were explored using cBioPortal.[16]

Prediction of INHBA regulatory miRNAs

MiRwalk and MicroT-CDS databases have been used to predict *INHBA* regulatory miRNAs.[17,18] The probable *INHBA* regulatory miRNAs in HNSC were selected from a list of common miRNAs that were both downregulated in HNSC tissues compared to normal controls and predicted by two databases.

Gene set enrichment analysis

Gene set enrichment analysis (GSEA) with normalized enrichment score (NES) based on TCGA-HNSC data set was used to investigate the biological properties of *INHBA* in HNSC. The threshold was set at a false discovery rate (FDR) *q*-value and a *P* value of less than 0.05.

Cell culture

HNSC cell lines Cal27, Hsc3, and Um1 were maintained in Dulbecco's modified Eagle medium (DMEM), while human normal oral keratinocytes Hok were maintained in oral keratinocyte medium (OKM). All cell lines were supplemented with 10% fetal bovine serum (FBS), 100 U/mL streptomycin, and 100 U/mL penicillin. The cells were cultured at 37°C in a humidified incubator containing 5% CO_2.

Total RNA extraction and qRT-PCR analysis

Total RNA was extracted from Hok, Cal27, Hsc3, and Um1 cells using the Cell Total RNA Isolation Kit (Foregene). PrimeScript II First-Strand cDNA Synthesis Kit (Takara) was used to synthesize cDNA from 1 g of RNA. *GAPDH* was used as an internal reference for *INHBA*, and the relative mRNA level of *INHBA* was measured using the One Step TB Green PrimeScript PLUS RT-PCR Kit (Takara). The $2^{-\Delta\Delta Ct}$ method was used to calculate the relative repression of *INHBA*.[19] The following primers were used for quantitative reverse transcription polymerase chain reaction (qRT-PCR): *INHBA*, 5′-GGCAAGTTGCTGGATTATAGTG-3′ (forward) and 5′-CTGAGAGTTGGGTACATCCTTT-3′ (reverse) and *GAPDH*, 5′-GGAGCGAGATCCCTCCAAAAT-3′ (forward) and 5′-GGCTGTTGTCATACTTCTCATGG-3′ (reverse).

Invasion and migration assays

Cells (5×10^5 cells per well) were seeded in six-well plates. When the cell density reached 90%, a scratch was created with a 200-L tip perpendicular to the dorsal transverse line, which was then washed three times with PBS and continued to culture. To determine cell migration, scratches were observed and photographed at 0 and 24 h, and the procedure was performed three times. A Transwell system was used to detect tumor cell invasion capability. Briefly, cells were seeded in the upper chamber using a gelled Matrigel matrix, and DMEM containing 10% FBS was added to the bottom chamber. After culture at 37°C and 5% CO_2 for 24 h, cells on the bottom surface of the upper chamber were fixed with 4% paraformaldehyde, stained with 0.1% crystal violet solution, photographed under a microscope, and counted.

Statistical analysis

Student's *t*-test was performed to compare *INHBA* expression across clinicopathological groups. The diagnostic significance of *INHBA* in HNSC was determined using the receiver operating characteristic (ROC) curve, and the area under the curve (AUC) was calculated. Based on *INHBA* expression levels, patients with HNSC were classified into low- and high-expression groups, and the correlation with clinicopathological characteristics was assessed using Pearson's chi-square test. Kaplan–Meier (K–M) analysis and log-rank test were used to evaluate the overall survival (OS) and disease-free survival (DFS) between the low and high *INHBA* expression groups. To identify the independent predictors related to OS or DFS, the Cox proportional hazards model was applied, and the hazard ratios (HRs) with 95% confidence intervals (CIs) were calculated. Cox multivariate analysis was used to construct nomograms for OS and DFS. The model was derived using the following formula:

$$Probability\ of\ event\ at\ time\ t = S_0(t)^{\exp(\beta_1 x_1 + \beta_2 x_2 \ldots)}$$

where β is the regression coefficient and x is the covariate observed value; the baseline survival function, $S_0(t)$, was also calculated from the data. The variable axes of the nomogram were constructed using regression coefficients, and S_0 was employed in the translation from total points to the predicted probability. The model was effectively measured using the concordance index (C-index). In addition, the correlation between the *INHBA* DNA methylation level (or miRNA expression) and *INHBA* mRNA expression was explored using linear regression analysis. A one-way analysis of variance (ANOVA) was performed for multiple group comparisons. Statistical analysis was performed using *R* version 4.1.0, and a two-tailed P value < 0.05, was regarded as statistically significant. To control the FDR, the Benjamini–Hochberg method was applied to the *P* value to perform multiplicity correction.

Results

INHBA was overexpressed in HNSC compared to normal controls

To explore the expression profile of *INHBA*, GEPIA was used to review the expression pattern of *INHBA* at the mRNA level in both tumor and normal tissues. The results showed upregulation of *INHBA* in various cancers, including BLCA, BRCA, COAD, ESCA, HNSC, PAAD, READ, and STAD (Figure 1(A)). We further focused on the expression of *INHBA* in HNSC. The expression of *INHBA* in HNSC tissues ($n = 495$) was significantly higher than that in the normal controls ($n = 44$) (Figure 1(B)), which was consistent with the *INHBA* expression pattern *in vitro* (Figure 1(C)). In addition, an ROC curve was applied to confirm the diagnostic significance of *INHBA* upregulation in HNSC, the results of which showed a strong predictive ability (AUC = 0.929, $p < 0.0001$) (Figure 1(D)).

INHBA overexpression was associated with tumor progression in HNSC

After investigating the *INHBA* expression pattern and its diagnostic value in HNSC, we sought to explore the clinical implications of *INHBA* based on the low- and high-expression groups. As shown in Table 1, although there were no significant differences in age ($p > 0.05$), *INHBA* overexpression was significantly associated with sex, tumor–node–metastasis (TNM) stage, histologic grade, human papillomavirus (HPV) status, OS, and DFS ($p < 0.05$). To increase the reliability of the results, we further analyzed *INHBA* mRNA expression data as a continuous variable in different subgroups, the results of which were consistent with previous findings (Figure 2(A) to (F)). We next conducted migration (Figure 2(G)) and invasion (Figure 2(H)) assays to determine the relationship between *INHBA* expression and HNSC metastatic ability *in vitro*. We found that the number of invaded and migrated cancer cells increased with *INHBA* expression among Cal27, Hsc3, and Um1 cells, indicating a positive correlation between *INHBA* and tumor metastasis, which might further lead to poor outcomes in patients with HNSC.

INHBA overexpression independently predicted poor OS and DFS in HNSC

We then assessed the prognostic value of *INHBA* in HNSC using the K–M curves. Patients with HNSC with high *INHBA* expression exhibited a lower OS (HR = 1.697, $p < 0.05$) and DFS (HR = 1.742, $p < 0.05$) (Figure 3(A) and (D)). Considering the patient heterogeneity between the

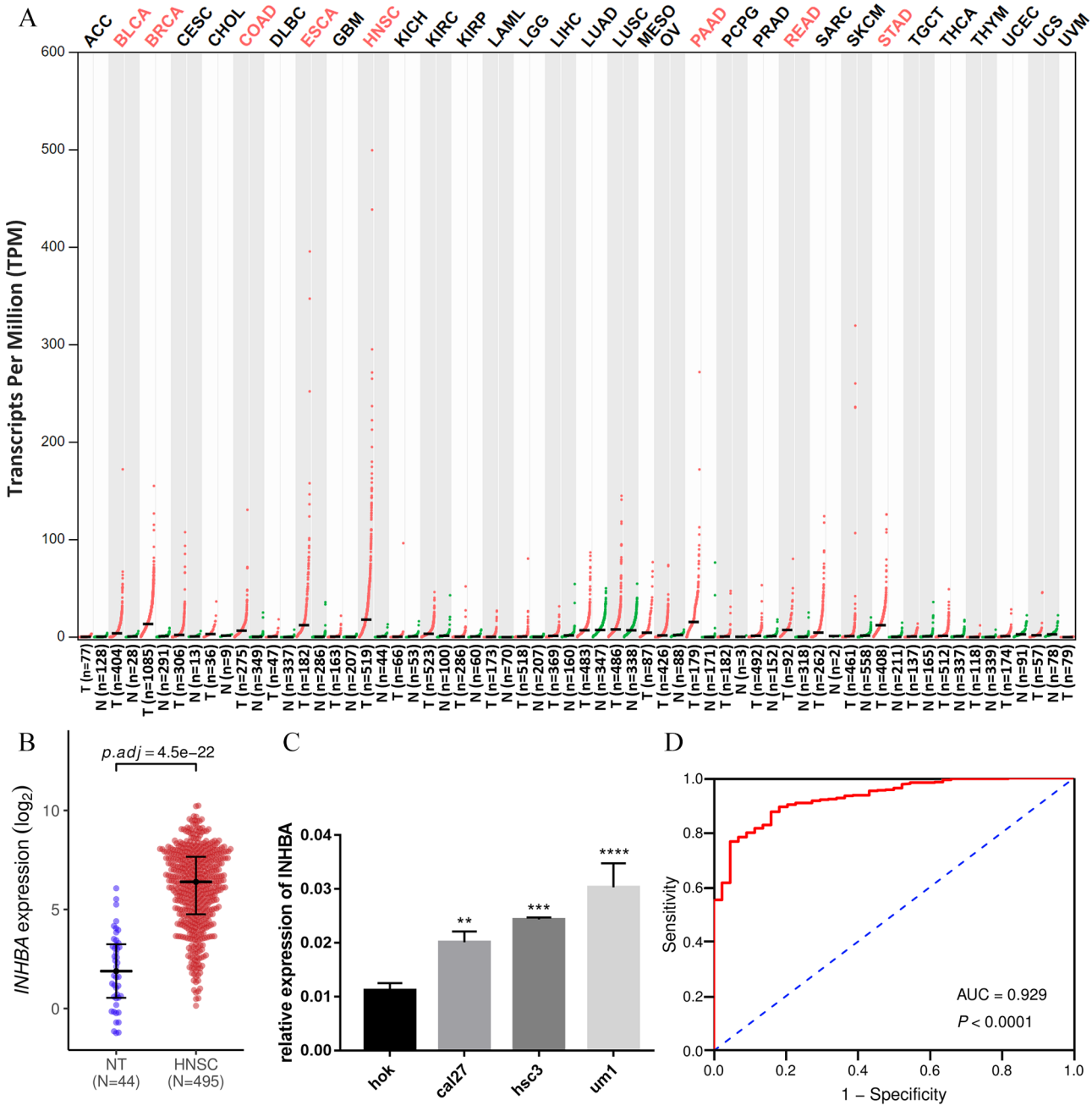

Figure 1. *INHBA* is significantly overexpressed in HNSC, both *in vitro* and *in vivo*: (A) Expression of *INHBA* in various tumor types and paired normal tissues. (B) Comparison of *INHBA* expression in HNSC ($n = 495$) and normal controls ($n = 44$). (C) Comparison of *INHBA* expression in HNSC cell lines (Cal27, Hsc3, and Um1) and human normal oral keratinocytes (Hok). (D) Validation of the diagnostic value of *INHBA* overexpression in HNSC using ROC curve. (A color version of this figure is available in the online journal.)
*$p<0.05$, **$p<0.01$, and ***$p<0.001$.

low- and high-expression groups, we further performed subgroup analysis based on the TNM stage. *INHBA* overexpression was consistently associated with unfavorable OS (HR = 1.953, $p < 0.05$) and DFS (HR = 1.872, $p < 0.05$) in stages III–IV patients (Figure 3(C) and (F)), while there was no significant difference in stages I–II patients ($p > 0.05$), suggesting that the *INHBA* expression level has a higher prognostic value in advanced HNSC (Figure 3(B) and (E)). In addition, Cox regression analysis was used to investigate the independent predictors of OS in HNSC (Table 2). The univariate model showed that age, sex, TNM stage, and *INHBA* expression level were significantly associated with OS in HNSC ($p < 0.05$). Furthermore, multivariate analysis indicated that *INHBA* overexpression in HNSC was an independent predictor of poor OS (HR = 1.140, $p < 0.05$) after adjusting for other prognostic predictors.

Validation of the prognostic value of INHBA using a nomogram in HNSC

Next, we sought to validate the prognostic value of *INHBA* in HNSC by constructing a nomogram based on age, TNM stage, and *INHBA* mRNA expression, all of which were independent predictors of OS in HNSC (Figure 4(A)). As shown in

Table 1. Association between INHBA expression and the clinical parameters in HNSC patients.

Variables	Total	INHBA expression		*P* value
		High	Low	
Age (year)				
<65	306	199	107	
⩾65	188	122	66	0.975
Gender				
Male	362	224	138	
Female	132	97	35	**0.0222**
TNM stage				
I	24	16	8	
II	72	47	25	
III	78	52	26	
IV	256	177	79	
Unknown	64	29	35	**0.0115**
Histologic grade				
G1–G2	355	246	109	
G3–G4	120	66	54	
Unknown	19	9	10	**0.00464**
HPV status				
Negative	72	55	17	
Positive	30	2	28	<**0.001**
Overall survival				
Alive	281	162	119	
Dead	213	159	54	<**0.001**
Disease-free survival				
Alive	344	208	136	
Dead	125	94	31	
Unknown	25	1	6	**0.00624**

INHBA: inhibin subunit βA; TNM: tumor–node–metastasis; HPV: human papillomavirus.
Statistically significant *P* values are given in bold.

the calibration plot, a high agreement was found between the actual observation and the nomogram prediction in terms of the survival probability (1-, 3-, and 5-year OS) (Figure 4(B)). The C-index of the nomogram for OS based on age, TNM stage, and *INHBA* mRNA expression was 0.616, and the 95% CI was 0.593–0.640, which was considerably higher than the C-index of the TNM staging alone (C-index: 0.568, 95% CI: 0.549–0.588).

INHBA overexpression in HNSC was attributed to DNA copy number gain and downregulation of miR-217-5p

The potential mechanisms underlying *INHBA* overexpression in HNSC were evaluated in terms of genetic and epigenetic alterations. In the following study, 514 patients with full mRNA, CNA, and methylation data were chosen, among which, 187 patients had different degrees of *INHBA* amplification (183 copy number gain and four amplification) compared to diploid, indicating the critical role of DNA amplification in *INHBA* upregulation (Figure 5(A)). The relationship between *INHBA* expression and DNA methylation was further evaluated by linear regression analysis, which showed a negative correlation ($r = -0.51$, $p < 0.0001$) (Figure 5(B)).

To reveal the epigenetic alterations in *INHBA* upregulation, we further identified the potential regulatory miRNAs of *INHBA*. The prediction cohort included miRNAs predicted using both MiRwalk and MicroT-CDS databases. Meanwhile, the miRNAs that were downregulated in HNSC were included in the HNSC cohort. The miRNAs that were common to the two cohorts were subsequently identified as probable *INHBA* regulatory miRNAs in HNSC. Finally, we identified 11 regulatory miRNAs, and selected miR-217-5p as a candidate for further validation because of its well-known role in cancer development (Figure 5(C)). We found that miR-217-5p was significantly downregulated in HNSC ($n = 518$) compared to that in the normal controls ($n = 44$) ($p < 0.0001$) (Figure 5(D)). Furthermore, a significant negative correlation between the expression of *INHBA* and miR-217-5p was found ($r = -0.21$, $p < 0.0001$), which was consistent with the regulatory relationship between miRNAs and their target genes (Figure 5(E)). In addition, the putative binding site of the *INHBA* 3′-untranslated region (UTR) by miR-217-5p was predicted using ENCORI,[20] which further improved the reliability of their interaction (Figure 5(F)). Taken together, our findings revealed that elevated *INHBA* expression is correlated with genetic and epigenetic alterations in HNSC.

GSEA and correlation between TP53 mutation and INHBA expression in HNSC

GSEA was used to investigate the biological roles of *INHBA* upregulation in HNSC, and showed that the following processes were significantly enriched: focal adhesion, extracellular matrix (ECM) receptor interaction, pathways in cancer, regulation of actin cytoskeleton, TGFβ signaling pathway, and ubiquitin-mediated proteolysis (Figure 6(A) to (F)). Considering the significance of *TP53* mutations in cancer,

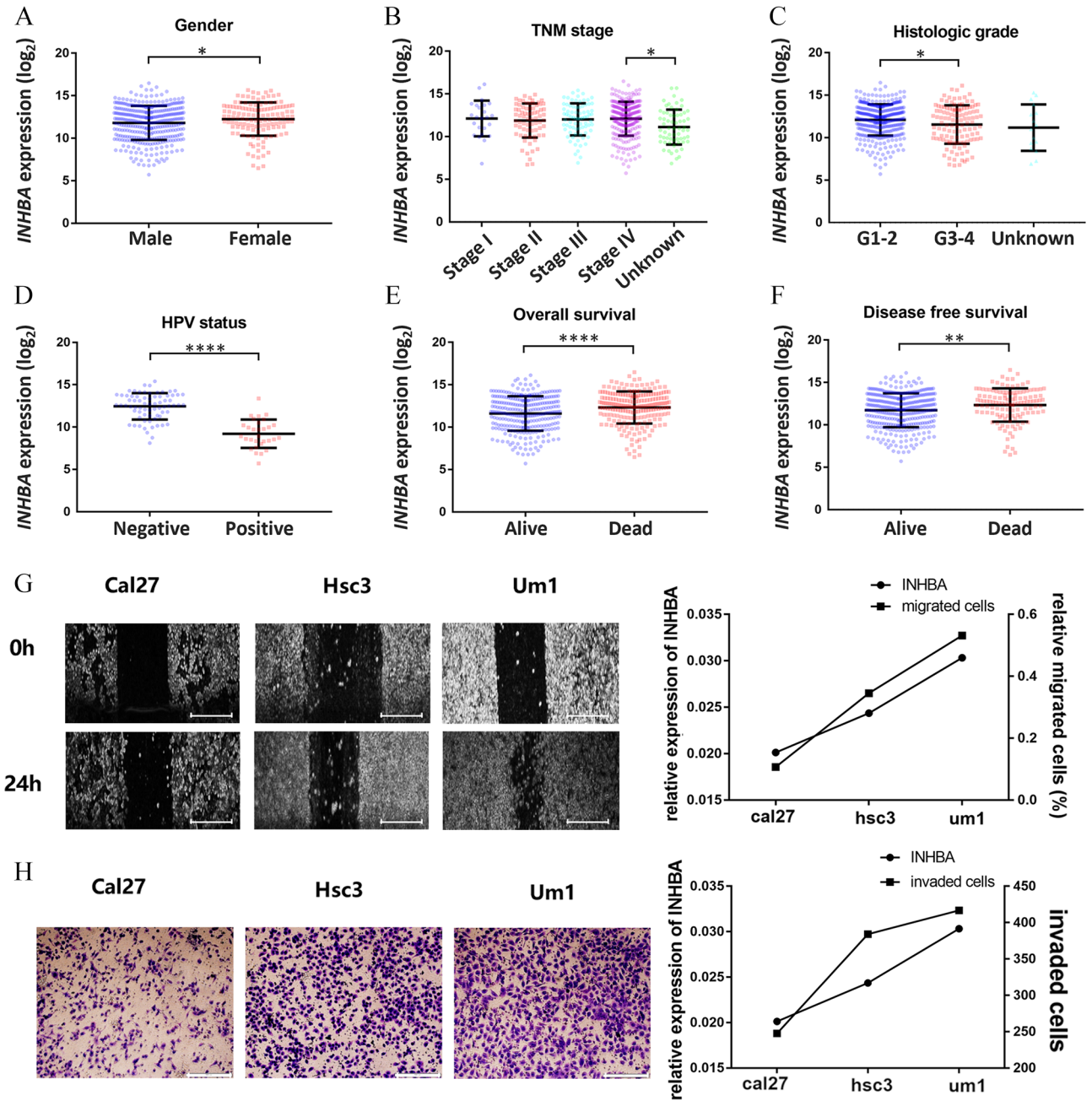

Figure 2. Subgroup analysis of *INHBA* expression in HNSC: Comparison of *INHBA* expression according to (A) sex, (B) TNM stage, (C) histologic grade, (D) HPV status, (E) OS, and (F) DFS. The relationship between *INHBA* expression and HNSC metastatic ability revealed by (G) migration and (H) invasion assays. *$p<0.05$, **$p<0.01$, and ***$p<0.001$. Scale bars represent 500 μm in (G) and 200 μm in (H).

we further studied the association between *INHBA* upregulation and *TP53* mutations in HNSC. The heat map shows that various genetic alterations in *TP53* were accompanied by *INHBA* overexpression (Figure 7(A)), and *INHBA* expression was significantly higher in the *TP53* mutation group ($p < 0.05$) (Figure 7(B) and (C)). In addition, unfavorable OS and DFS were also correlated with *TP53* mutations in patients with HNSC ($p < 0.05$) (Figure 7(D) and (E)).

Discussion

HNSC is a worldwide health problem with an unfavorable prognosis. Although a decline in the incidence of HNSC is expected globally, in part because of the decreased use of tobacco, it may not be evident until after 2060.[21,22] Accumulation of genetic aberrations affecting cellular processes, such as DNA repair, inflammation, proliferation, apoptosis, and angiogenesis, may contribute to HNSC formation by improving susceptibility to tumor development.[23] As a result, it is critical to uncover genetic markers for the early detection of HNSC as well as novel targets to develop new therapeutic techniques. TGFβ signaling maintains epithelial homeostasis by regulating cell cycle progression, differentiation, apoptosis, and adhesion; thus, defective TGFβ signaling is extensively found in many malignancies, including HNSC.[24] Of the ligands in TGFβ superfamily signaling,

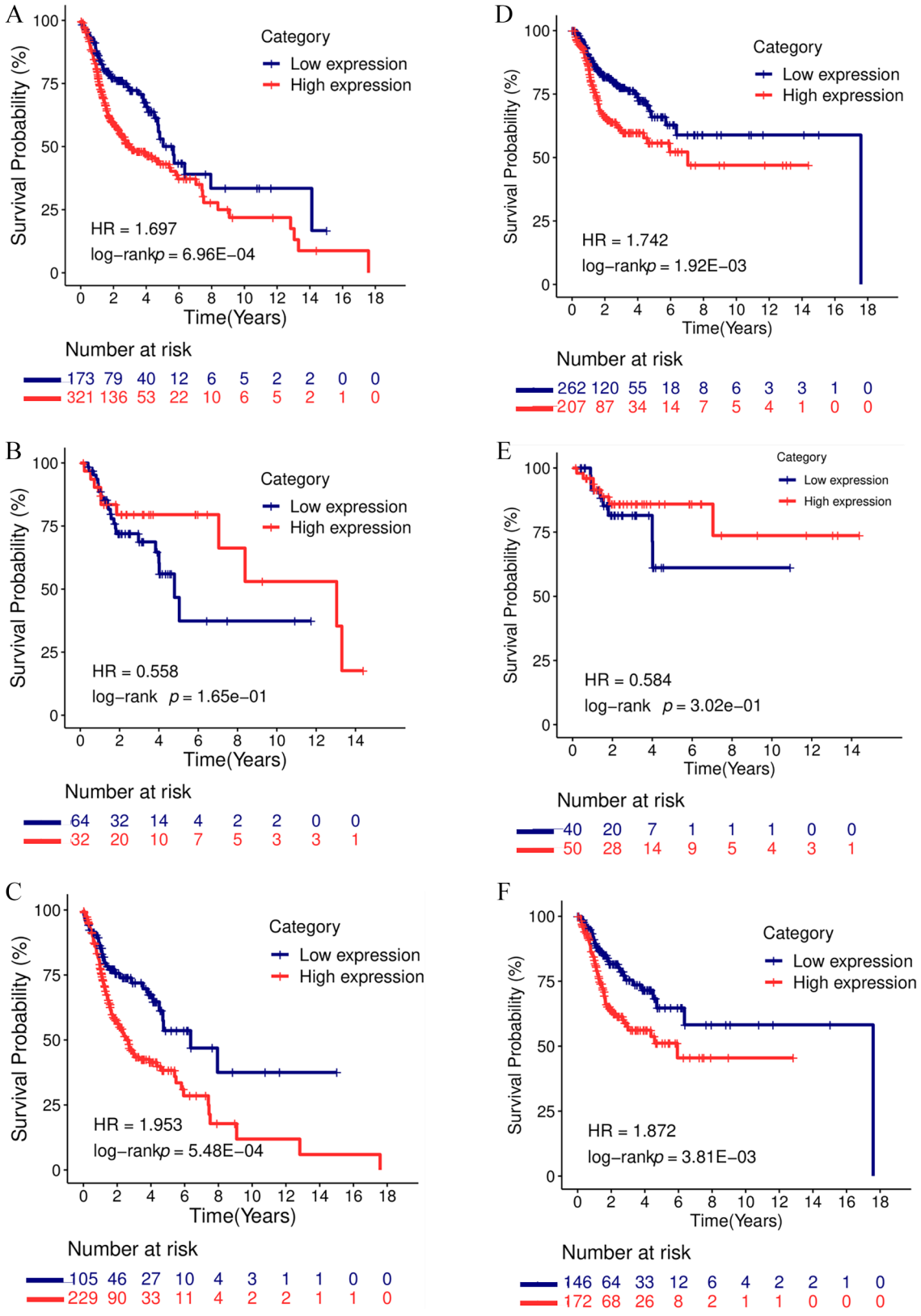

Figure 3. K–M survival analysis based on the *INHBA* expression level in HNSC. K–M curves of (A) OS and further subgroup analysis based on TNM (B) stages I–II and (C) stages III–IV patients. (D) K–M curves of DFS, and further subgroup analysis based on TNM (E) stages I–II and (F) stages III–IV patients.

TGFβ and bone morphogenic proteins (BMPs) have been extensively studied in terms of their functions in cancer, particularly regarding epithelial–mesenchymal transition (EMT), and tumor cell migration and invasion. However, activin A signaling is less well understood, and few studies have investigated the role of *INHBA* in HNSC. Despite the structural similarity between TGFβ and activin A, TGFβ is released as a dormant precursor that must be activated,

Table 2. Cox proportional hazards regression model analysis of OS.

Variables	Univariate analysis		Multivariate analysis	
	HR (95% CI)	*P* value	HR (95% CI)	*P* value
Age (⩾65 vs <65)	1.39 (1.06, 1.83)	**0.017**	1.47 (1.11, 1.95)	**0.007**
Gender (Female vs male)	1.34 (1, 1.79)	**0.048**	1.27 (0.94, 1.71)	0.116
TNM stage (II vs I)	1.9 (0.67, 5.43)	0.230	–	–
TNM stage (III vs I)	2.13 (0.75, 6.08)	0.158	–	–
TNM stage (IV vs I)	3.32 (1.23, 8.99)	**0.018**	3.65 (1.35, 9.9)	**0.011**
Histologic grade (G3–G4 vs G1–G2)	0.96 (0.7, 1.31)	0.806	–	–
HPV status (positive vs negative)	0.49 (0.17, 1.43)	0.193	–	–
INHBA (high vs low)	1.12 (1.04, 1.21)	**0.002**	1.14 (1.06, 1.23)	**0.001**

HR: hazard ratio; CI: confidence interval; INHBA: inhibin subunit βA; TNM: tumor–node–metastasis; HPV: human papillomavirus.
Statistically significant *P* values are given in bold.

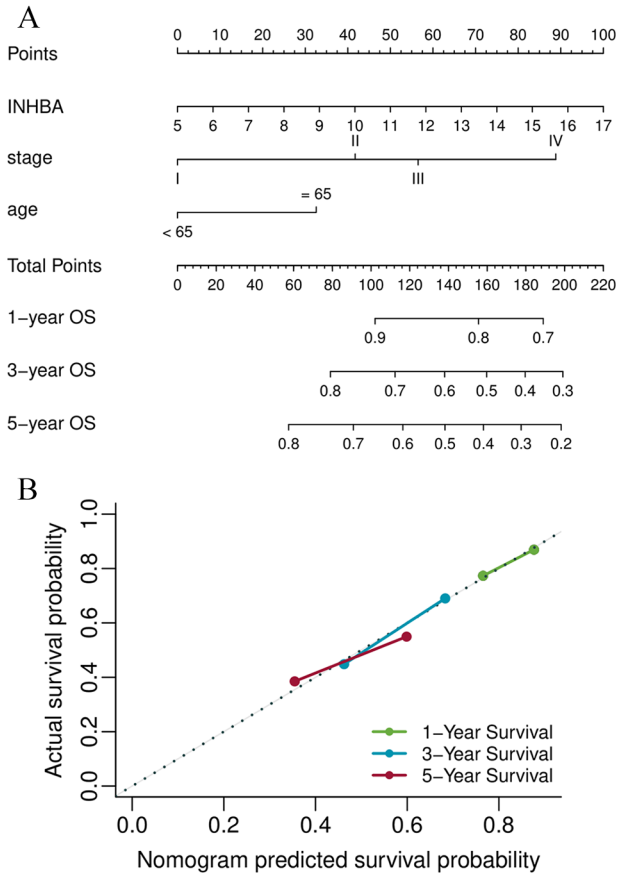

Figure 4. Validation of the *INHBA* prognostic value in HNSC based on nomogram: (A) Prognostic nomogram for patients with HNSC, and (B) the calibration curve of the nomogram for predicting OS.

whereas activin A is released as a fully functional protein, which operates through different downstream transcriptional targets, as well as overlapping Smad-dependent pathways, resulting in distinct functional consequences. In HNSC, tumor-associated myofibroblasts (TAMs) secrete increased levels of activin A, which are related to positive lymph node status and unfavorable prognosis.[25–28] In addition, OSCC cells overexpress activin A in an autocrine manner to regulate invasiveness, proliferation, and apoptosis of tumor cells.[26,29] Thus, activin A overexpression can be regarded as an independent prognostic marker of survival.[26,30,31] Considering the importance of *INHBA* in regulating activin A signaling, it has long been considered a potential therapeutic target for HNSC, more than simply a basic marker of tumor progression. Nevertheless, the underlying mechanism of *INHBA* in HNSC is yet to be fully elucidated.

In this study, we discovered that *INHBA* was significantly elevated in patients with HNSC compared to normal controls, and the ROC curves demonstrated high diagnostic value. These findings suggest that *INHBA* could be a promising biomarker for the pathological and molecular diagnosis of HNSC. We also evaluated the clinical implications of *INHBA* overexpression in HNSC. It was demonstrated that *INHBA* upregulation was correlated with sex, TNM stage, histologic grade, HPV status, OS, and DFS, suggesting that *INHBA* plays a role in the tumorigenesis and progression of HNSC. Meanwhile, K–M analysis demonstrated that patients with HNSC with increased *INHBA* expression exhibited worse OS and DFS. The *in vitro* experiment further showed that cancer cell invasion and migration were positively correlated with *INHBA* expression, indicating the important role of *INHBA* in HNSC progression and poor outcome. Furthermore, multivariate analysis also showed that *INHBA* upregulation was an independent predictor of relatively poor OS and DFS in patients with HNSC. Considering the remarkable heterogeneity of individual patients with HNSC, we sought to compare the prognostic value of *INHBA* and the well-established TNM staging system. Here, we constructed a nomogram based on TNM stage and *INHBA* mRNA expression in patients with HNSC, which demonstrated that the genomic–clinicopathologic nomogram could predict survival more precisely than the TNM staging system alone. Taken together, these findings suggest that *INHBA* may be a promising prognostic factor for HNSC, which may help to improve clinical decisions.

In addition to exploring the prognostic value of *INHBA* in HNSC, we further attempted to explain the underlying mechanisms of *INHBA* overexpression in HNSC from two aspects: genetic and epigenetic alterations. We observed that 36.4% (187/514) of patients with HNSC showed low- or high-level *INHBA* DNA amplification, which was significantly associated with *INHBA* overexpression. Furthermore, considering the contribution of DNA hypomethylation to chromosomal instability and gene dysregulation in a variety of malignancies,[32] the promoter methylation level of *INHBA* was also investigated. Consistent with our expectation, there was a strong association between *INHBA* overexpression

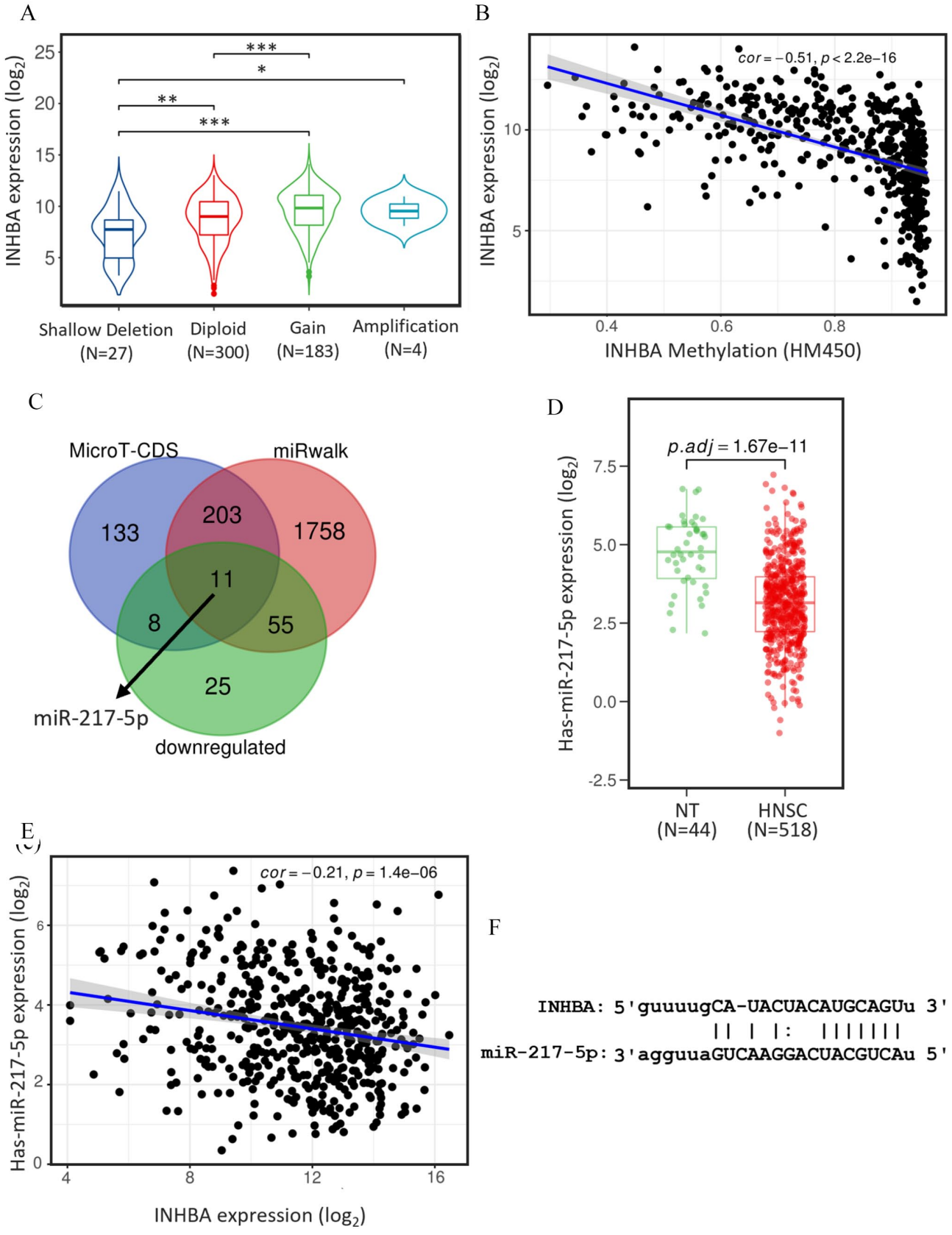

Figure 5. DNA copy number gain and downregulated miR-217-5p contribute to *INHBA* overexpression in HNSC: (A) Comparison of *INHBA* expression in different CNA groups. (B) Correlation analysis between *INHBA* expression and *INHBA* DNA methylation. (C) Prediction of *INHBA* regulatory miRNAs based on MiRwalk, MicroT-CDS, and downregulated miRNAs in HNSC. (D) Expression of miR-217-5p in HNSC ($n = 518$) compared to normal controls ($n = 44$). (E) Correlation analysis between *INHBA* and miR-217-5p expression in HNSC. (F) Putative binding site of *INHBA* 3′-UTR by miR-217-5p. (A color version of this figure is available in the online journal.)

*$p < 0.05$, **$p < 0.01$, and ***$p < 0.001$.

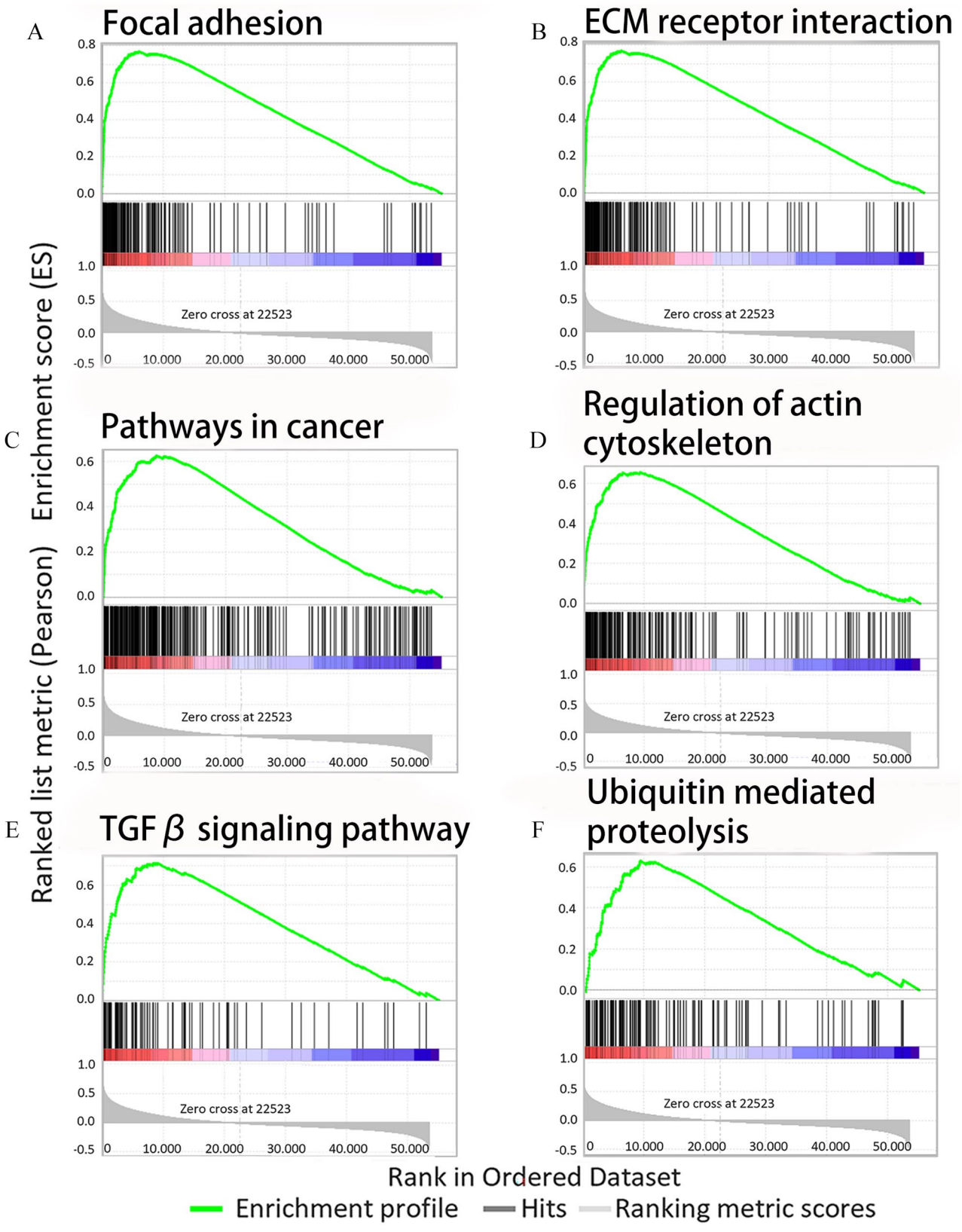

Figure 6. GSEA using TCGA-HNSC data set: *INHBA* upregulation was significantly correlated with (A) focal adhesion, (B) ECM receptor interaction, (C) pathways in cancer, (D) regulation of actin cytoskeleton, (E) TGFβ signaling pathway, and (F) ubiquitin-mediated proteolysis. (A color version of this figure is available in the online journal.)

and DNA hypomethylation in HNSC, suggesting that post-translational modification may play a role in the alteration of *INHBA* expression. As another type of epigenetic alteration other than DNA hypomethylation, miRNA-regulated mRNA degradation also has an influence on gene dysregulation.[33] By screening the potential regulatory miRNAs of *INHBA*,

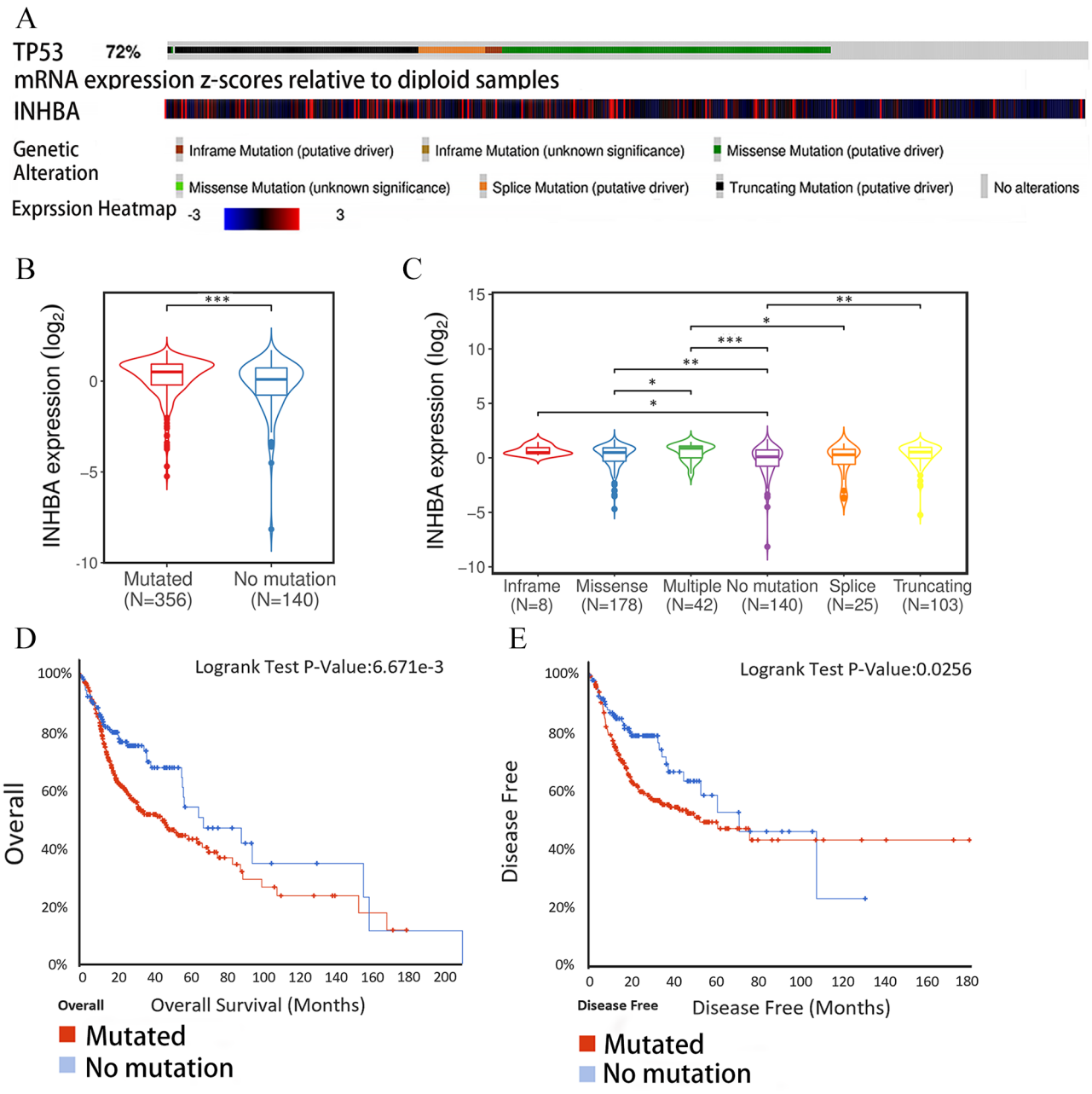

Figure 7. *INHBA* upregulation may be correlated with *TP53* mutation in HNSC: (A) Heat map of *INHBA* expression and the genetic alteration of *TP53* in TCGA-HNSC data set. (B) Comparison of *INHBA* expression between the *TP53* mutation group and the *TP53* wild type group. (C) Comparison of *INHBA* expression according to *TP53* mutation status. *TP53* mutation is correlated with poor (D) OS and (E) DFS. *$p < 0.05$, ** $p < 0.01$, and ***$p < 0.001$.

miR-217-5p was found to be significantly downregulated in HNSC compared to normal controls, and its expression was negatively correlated with *INHBA* expression. Furthermore, the potential binding location of the *INHBA* 3′-UTR to miR-217-5p supported the hypothesis that miR-217-5p is an upstream regulator of *INHBA* in HNSC. In summary, the data above imply that *INHBA* overexpression in HNSC may be explained in part by DNA copy number gain, *INHBA* promoter hypomethylation, and downregulation of miR-217-5p.

Previous studies have not thoroughly investigated the biological roles of *INHBA* overexpression in HNSC. It has been demonstrated that high *INHBA* expression in HNSC is related to focal adhesion, ECM receptor interaction, pathways in cancer, regulation of actin cytoskeleton, TGFβ signaling pathway, and ubiquitin-mediated proteolysis, all of which have been demonstrated to play a role in tumorigenesis and progression.[24,34] Intriguingly, TGFβ has been found to have different, even opposite effects on tumor cells under different conditions. In the early stage of tumorigenesis, TGFβ predominantly functions as a tumor suppressor by promoting the expression of cyclin-dependent kinase inhibitors (p15, p21, p57, and 4E-BP1) to induce cell cycle arrest.[35,36] However, cancer cells gradually adapt to the suppressive functions of TGFβ. In the malignant stage, TGFβ can produce ECM to create a beneficial tumor microenvironment (TME) in a paracrine manner.[37] In addition, tumor cells utilize TGFβ to obtain a growth advantage and promote EMT, which causes epithelial tumor cells to lose their ability to adhere, while also

facilitating their migration and invasion by inhibiting the expression of occludin, E-cadherin, and ZO-1.[38,39] The dual roles of TGFβ in cancer progression may partly explain why *INHBA* upregulation is only significantly associated with poor OS and DFS in advanced HNSC (Figure (C) and (F)). In addition, the TGF-β pathway is tightly regulated. E3 ubiquitin ligases, including NEDD4-2, WWP1, and SMURF1/2, can be recruited by SMAD7 to degrade TGFβRI in an ubiquitination-mediated proteasomal and/or lysosomal manner.[40–42] Ubiquitin-specific proteases (USPs) are cysteine-dependent proteases, which constitute the largest subfamily of deubiquitinating enzymes and can reverse the ubiquitination of TGFβRI.[43,44] Given the significant roles of the TGFβ superfamily in regulating numerous tumor cell functions, TGF-neutralizing antibodies and ligand traps that impede TGF binding to its receptors, as well as selective small-molecule TGF receptor kinase inhibitors, have demonstrated promising therapeutic potential in antitumor treatments.[45,46] However, considering the highly pleiotropic functions of TGFβ, systemic inhibition of TGFβ can also affect normal cells other than the tumor itself, leading to safety concerns and adverse effects. Therefore, *INHBA* may be a potential biomarker for selecting patients who will benefit most from anti-TGFβ treatments. To further consolidate the diagnostic value of *INHBA*, we sought to explore the correlation between *INHBA* overexpression and *TP53* mutations in HNSC. Genome instability is the underlying mechanism of various cancer hallmarks, including unstrained replicative immortality, resistance to apoptosis, and uncontrolled cell proliferation.[47] P53 protein, encoded by the *TP53* gene, has been extensively researched as a key tumor suppressor in most cancer types. Focusing specifically on HNSC, large-scale whole-genome sequencing studies have also confirmed frequent disruptive mutations of *TP53*, which have been associated with poor prognosis and resistance to therapy.[48,49] We found that 71.8% (356/496) of patients in TCGA-HNSC data set had *TP53* mutations, which were associated with considerably higher *INHBA* expression levels and poor OS and DFS in HNSC.

In conclusion, *INHBA* expression was considerably higher in HNSC tissues than in normal controls, which could be attributed to *INHBA* DNA copy number gain and downregulation of miR-217-5p in HNSC. In addition, *INHBA* overexpression was associated with tumor progression and independently predicted poor OS and DFS in patients with HNSC, which was verified *in vitro* by migration and invasion assays. Furthermore, *INHBA* upregulation was significantly associated with focal adhesion, ECM receptor interaction, pathways in cancer, regulation of actin cytoskeleton, TGFβ signaling pathway, and ubiquitin-mediated proteolysis. We conclude that using *INHBA* as a predictive biomarker to select patients with HNSC who will benefit the most from anti-TGFβ therapy may be a potential treatment for HNSC. Further research is needed to determine the precise mechanism of *INHBA* in HNSC through validation in clinical samples and *in vivo* experiments.

AUTHORS' CONTRIBUTIONS

WBY, SHZ, and TLL contributed to the conception and design; SHZ, KYJ, TLL, and MLZ conducted the experiments; SHZ analyzed the data and wrote the manuscript; KYJ, TLL, and MLZ generated the figures; and WBY critically reviewed, edited, and approved the manuscript. All authors read and approved the final manuscript.

ACKNOWLEDGEMENTS

The authors thank Dr Huandi Qiu, Dr Yuexia Yin, Dr Nan Wang, Dr Lingyun Zhang, and Dr Qingqing Li (State Key Laboratory of Biotherapy, West China Hospital, Sichuan University) for their assistance with the experiments, and Dr Jianming Zeng (University of Macau) for generously sharing his experiences and codes.

DECLARATION OF CONFLICTING INTERESTS

The author(s) declared no potential conflicts of interest with respect to the research, authorship, and/or publication of this article.

FUNDING

The author(s) disclosed receipt of the following financial support for the research, authorship, and/or publication of this article: This work was supported by grants from the Sichuan University-Panzhihua City 2021 Campus Cooperation Special Fund Project (grant number 2021CDPZH-7), the Research and Development Foundation of West China Hospital of Stomatology, Sichuan University (grant number RD-02-201907), and the College Students' Innovative Entrepreneurial Training Plan Program (grant number 202110610169).

ORCID ID

Wenbin Yang https://orcid.org/0000-0001-5348-7906

REFERENCES

1. Siegel RL, Miller KD, Jemal A. Cancer statistics, 2019. *CA Cancer J Clin* 2019;**69**:7–34
2. Bray F, Ferlay J, Soerjomataram I, Siegel RL, Torre LA, Jemal A. Global cancer statistics 2018: GLOBOCAN estimates of incidence and mortality worldwide for 36 cancers in 185 countries. *CA Cancer J Clin* 2018;**68**:394–424
3. Chow LQM. Head and neck cancer. *N Engl J Med* 2020;**382**:60–72
4. Bose P, Brockton NT, Dort JC. Head and neck cancer: from anatomy to biology. *Int J Cancer* 2013;**133**:2013–23
5. Owens P, Engelking E, Han G, Haeger SM, Wang XJ. Epidermal Smad4 deletion results in aberrant wound healing. *Am J Pathol* 2010;**176**:122–33
6. Massague J. TGFbeta in cancer. *Cell* 2008;**134**:215–30
7. Ikushima H, Miyazono K. TGFbeta signalling: a complex web in cancer progression. *Nat Rev Cancer* 2010;**10**:415–24
8. Kwon HE, Jia S, Lan Y, Liu H, Jiang R. Activin and Bmp4 signaling converge on Wnt activation during odontogenesis. *J Dent Res* 2017;**96**:1145–52
9. Wijayarathna R, de Kretser DM, Sreenivasan R, Ludlow H, Middendorff R, Meinhardt A, Loveland KL, Hedger MP. Comparative analysis of activins A and B in the adult mouse epididymis and vas deferens. *Reproduction* 2018;**155**:15–23
10. Hashimoto O, Yamato K, Koseki T, Ohguchi M, Ishisaki A, Shoji H, Nakamura T, Hayashi Y, Sugino H, Nishihara T. The role of activin type I receptors in activin A-induced growth arrest and apoptosis in mouse B-cell hybridoma cells. *Cell Signal* 1998;**10**:743–9
11. Chang WM, Lin YF, Su CY, Peng HY, Chang YC, Lai TC, Wu GH, Hsu YM, Chi LH, Hsiao JR, Chen CL, Chang JY, Shieh YS, Hsiao M, Shiah SG. Dysregulation of RUNX2/activin-A axis upon miR-376c downregulation promotes lymph node metastasis in head and neck squamous cell carcinoma. *Cancer Res* 2016;**76**:7140–50
12. Tsai CN, Tsai CL, Yi JS, Kao HK, Huang Y, Wang CI, Lee YS, Chang KP. Activin A regulates the epidermal growth factor receptor promoter by activating the PI3K/SP1 pathway in oral squamous cell carcinoma cells. *Sci Rep* 2019;**9**:5197

13. Wu ZH, Tang Y, Niu X, Cheng Q. Expression and gene regulation network of INHBA in head and neck squamous cell carcinoma based on data mining. *Sci Rep* 2019;**9**:14341
14. Zhou S, Zhu C, Pang Q, Liu HC. MicroRNA-217: a regulator of human cancer. *Biomed Pharmacother* 2021;**133**:110943
15. Tang Z, Li C, Kang B, Gao G, Li C, Zhang Z. GEPIA: a web server for cancer and normal gene expression profiling and interactive analyses. *Nucleic Acids Res* 2017;**45**:W98–102
16. Cerami E, Gao J, Dogrusoz U, Gross BE, Sumer SO, Aksoy BA, Jacobsen A, Byrne CJ, Heuer ML, Larsson E, Antipin Y, Reva B, Goldberg AP, Sander C, Schultz N. The cBio cancer genomics portal: an open platform for exploring multidimensional cancer genomics data. *Cancer Discov* 2012;**2**:401–4
17. Sticht C, De La Torre C, Parveen A, Gretz N. miRWalk: an online resource for prediction of microRNA binding sites. *PLoS ONE* 2018;**13**:e0206239
18. Paraskevopoulou MD, Georgakilas G, Kostoulas N, Vlachos IS, Vergoulis T, Reczko M, Filippidis C, Dalamagas T, Hatzigeorgiou AG. DIANA-microT web server v5.0: service integration into miRNA functional analysis workflows. *Nucleic Acids Res* 2013;**41**:W169–73
19. Livak KJ, Schmittgen TD. Analysis of relative gene expression data using real-time quantitative PCR and the 2(-Delta Delta C(T)) Method. *Methods* 2001;**25**:402–8
20. Li JH, Liu S, Zhou H, Qu LH, Yang JH. starBase v2.0: decoding miRNA-ceRNA, miRNA-ncRNA and protein-RNA interaction networks from large-scale CLIP-Seq data. *Nucleic Acids Res* 2014;**42**:D92–17
21. Gillison ML, Chaturvedi AK, Anderson WF, Fakhry C. Epidemiology of human papillomavirus-positive head and neck squamous cell carcinoma. *J Clin Oncol* 2015;**33**:3235–42
22. Global Burden of Disease Cancer C, Fitzmaurice C, Allen C, Barber RM, Barregard L, Bhutta ZA, Brenner H, Dicker DJ, Chimed-Orchir O, Dandona R, Dandona L, Fleming T, Forouzanfar MH, Hancock J, Hay RJ, Hunter-Merrill R, Huynh C, Hosgood HD, Johnson CO, Jonas JB, Khubchandani J, Kumar GA, Kutz M, Lan Q, Larson HJ, Liang X, Lim SS, Lopez AD, MacIntyre MF, Marczak L, Marquez N, Mokdad AH, Pinho C, Pourmalek F, Salomon JA, Sanabria JR, Sandar L, Sartorius B, Schwartz SM, Shackelford KA, Shibuya K, Stanaway J, Steiner C, Sun J, Takahashi K, Vollset SE, Vos T, Wagner JA, Wang H, Westerman R, Zeeb H, Zoeckler L, Abd-Allah F, Ahmed MB, Alabed S, Alam NK, Aldhahri SF, Alem G, Alemayohu MA, Ali R, Al-Raddadi R, Amare A, Amoako Y, Artaman A, Asayesh H, Atnafu N, Awasthi A, Saleem HB, Barac A, Bedi N, Bensenor I, Berhane A, Bernabe E, Betsu B, Binagwaho A, Boneya D, Campos-Nonato I, Castaneda-Orjuela C, Catala-Lopez F, Chiang P, Chibueze C, Chitheer A, Choi JY, Cowie B, Damtew S, das Neves J, Dey S, Dharmaratne S, Dhillon P, Ding E, Driscoll T, Ekwueme D, Endries AY, Farvid M, Farzadfar F, Fernandes J, Fischer FTTGH, Gebru A, Gopalani S, Hailu A. Global, regional, and national cancer incidence, mortality, years of life lost, years lived with disability, and disability-adjusted life-years for 32 cancer groups, 1990 to 2015: a systematic analysis for the Global Burden of Disease Study. *JAMA Oncol* 2017; **3**: 524–48
23. Mao L, Hong WK, Papadimitrakopoulou VA. Focus on head and neck cancer. *Cancer Cell* 2004;**5**:311–6
24. Batlle E, Massague J. Transforming growth factor-beta signaling in immunity and cancer. *Immunity* 2019;**50**:924–40
25. Chang KP, Kao HK, Liang Y, Cheng MH, Chang YL, Liu SC, Lin YC, Ko TY, Lee YS, Tsai CL, Wang TH, Hao SP, Tsai CN. Overexpression of activin A in oral squamous cell carcinoma: association with poor prognosis and tumor progression. *Ann Surg Oncol* 2010;**17**:1945–56
26. Kelner N, Rodrigues PC, Bufalino A, Fonseca FP, Santos-Silva AR, Miguel MC, Pinto CA, Leme AF, Graner E, Salo T, Kowalski LP, Coletta RD. Activin A immunoexpression as predictor of occult lymph node metastasis and overall survival in oral tongue squamous cell carcinoma. *Head Neck* 2015;**37**:479–86
27. Sobral LM, Bufalino A, Lopes MA, Graner E, Salo T, Coletta RD. Myofibroblasts in the stroma of oral cancer promote tumorigenesis via secretion of activin A. *Oral Oncol* 2011;**47**:840–6
28. Bhowmick NA, Chytil A, Plieth D, Gorska AE, Dumont N, Shappell S, Washington MK, Neilson EG, Moses HL. TGF-beta signaling in fibroblasts modulates the oncogenic potential of adjacent epithelia. *Science* 2004;**303**:848–51
29. Bufalino A, Cervigne NK, de Oliveira CE, Fonseca FP, Rodrigues PC, Macedo CC, Sobral LM, Miguel MC, Lopes MA, Paes Leme AF, Lambert DW, Salo TA, Kowalski LP, Graner E, Coletta RD. Low miR-143/miR-145 cluster levels induce activin A overexpression in oral squamous cell carcinomas, which contributes to poor prognosis. *PLoS ONE* 2015;**10**:e0136599
30. Ogawa K, Funaba M. Activin in humoral immune responses. *Vitam Horm* 2011;**85**:235–53
31. Ervolino De Oliveira C, Dourado MR, Sawazaki-Calone I, Costa De Medeiros M, Rossa Junior C, De Karla Cervigne N, Esquiche Leon J, Lambert D, Salo T, Graner E, Coletta RD. Activin A triggers angiogenesis via regulation of VEGFA and its overexpression is associated with poor prognosis of oral squamous cell carcinoma. *Int J Oncol* 2020;**57**:364–76
32. Eden A, Gaudet F, Waghmare A, Jaenisch R. Chromosomal instability and tumors promoted by DNA hypomethylation. *Science* 2003;**300**:455
33. Zhang S, Gong Y, Li C, Yang W, Li L. Beyond regulations at DNA levels: a review of epigenetic therapeutics targeting cancer stem cells. *Cell Prolif* 2021;**54**:e12963
34. Xie F, Ling L, van Dam H, Zhou F, Zhang L. TGF-beta signaling in cancer metastasis. *Acta Biochim Biophys Sin* 2018;**50**:121–32
35. Azar R, Alard A, Susini C, Bousquet C, Pyronnet S. 4E-BP1 is a target of Smad4 essential for TGFbeta-mediated inhibition of cell proliferation. *EMBO J* 2009;**28**:3514–22
36. Chen Z, Li DQ, Tong L, Stewart P, Chu C, Pflugfelder SC. Targeted inhibition of p57 and p15 blocks transforming growth factor beta-inhibited proliferation of primary cultured human limbal epithelial cells. *Mol Vis* 2006;**12**:983–94
37. Chen W, Ten Dijke P. Immunoregulation by members of the TGFbeta superfamily. *Nat Rev Immunol* 2016;**16**:723–40
38. Hao Y, Baker D, Ten Dijke P. TGF-beta-mediated epithelial-mesenchymal transition and cancer metastasis. *Int J Mol Sci* 2019;**20**:2767
39. Derynck R, Muthusamy BP, Saeteurn KY. Signaling pathway cooperation in TGF-beta-induced epithelial-mesenchymal transition. *Curr Opin Cell Biol* 2014;**31**:56–66
40. Kuratomi G, Komuro A, Goto K, Shinozaki M, Miyazawa K, Miyazono K, Imamura T. NEDD4-2 (neural precursor cell expressed, developmentally down-regulated 4-2) negatively regulates TGF-beta (transforming growth factor-beta) signalling by inducing ubiquitin-mediated degradation of Smad2 and TGF-beta type I receptor. *Biochem J* 2005;**386**:461–70
41. Komuro A, Imamura T, Saitoh M, Yoshida Y, Yamori T, Miyazono K, Miyazawa K. Negative regulation of transforming growth factor-beta (TGF-beta) signaling by WW domain-containing protein 1 (WWP1). *Oncogene* 2004;**23**:6914–23
42. Kavsak P, Rasmussen RK, Causing CG, Bonni S, Zhu H, Thomsen GH, Wrana JL. Smad7 binds to Smurf2 to form an E3 ubiquitin ligase that targets the TGF beta receptor for degradation. *Mol Cell* 2000;**6**:1365–75
43. Liu S, de Boeck M, van Dam H, Ten Dijke P. Regulation of the TGF-beta pathway by deubiquitinases in cancer. *Int J Biochem Cell Biol* 2016;**76**:135–45
44. Liu S, Gonzalez-Prieto R, Zhang M, Geurink PP, Kooij R, Iyengar PV, van Dinther M, Bos E, Zhang X, Le Devedec SE, van de Water B, Koning RI, Zhu HJ, Mesker WE, Vertegaal ACO, Ovaa H, Zhang L, Martens JWM, Ten Dijke P. Deubiquitinase activity profiling identifies UCHL1 as a candidate oncoprotein that promotes TGFbeta-induced breast cancer metastasis. *Clin Cancer Res* 2020;**26**:1460–73
45. Huynh LK, Hipolito CJ, Ten Dijke P. A Perspective on the development of TGF-beta inhibitors for cancer treatment. *Biomolecules* 2019;**9**:743
46. Colak S, Ten Dijke P. Targeting TGF-beta signaling in cancer. *Trends Cancer* 2017;**3**:56–71
47. Hanahan D, Weinberg RA. Hallmarks of cancer: the next generation. *Cell* 2011;**144**:646–74
48. Cancer Genome Atlas N. Comprehensive genomic characterization of head and neck squamous cell carcinomas. *Nature* 2015;**517**:576–82
49. Poeta ML, Manola J, Goldwasser MA, Forastiere A, Benoit N, Califano JA, Ridge JA, Goodwin J, Kenady D, Saunders J, Westra W, Sidransky D, Koch WM. TP53 mutations and survival in squamous-cell carcinoma of the head and neck. *N Engl J Med* 2007;**357**:2552–61

(Received December 10, 2021, Accepted February 14, 2022)